scientific reports

Check for updates

OPEN

Phylogenetic comparative analysis of functional morphology sheds light on the evolution of seasonal migration in nightingale-thrushes (Turdidae: *Catharus*)

Matthew R. Halley[1,2,3]✉, Therese A. Catanach[2], John Klicka[4] & Jason D. Weckstein[1,2]

This study investigates the evolution of locomotory morphology and migratory behavior in nightingale-thrushes (genus *Catharus*), a clade of songbirds with diverse migratory strategies. With large datasets of molecular and morphometric characters, we resolve phylogenetic relationships, identify and model migration-related morphological characters, and estimate ancestral states of those characters to infer evolutionary transitions in the migratory phenotype. While acknowledging that unknown factors (e.g., differential extinction) may confound interpretation, our results suggest that (1) migratory behavior and its functional morphology are fundamentally linked; (2) short-distance or elevational migration (not long-distance) was the ancestral state of *Catharus*; (3) short-distance migration was the evolutionary precursor of long-distance migration; and (4) the short-distance migrant, Hermit Thrush (*C. guttatus*), may be in relative phenotypic (ecological) stasis. This potentially explains the ecological incumbency of *C. guttatus* in temperate North America during winter, and offers a new framework for interpreting the evolutionary sequence that produced long-distance migration in this model system.

Keywords Ancestral states, Macroevolution, Locomotion, Long-distance migration, Stasis, UCEs

In most animals, the functional morphology of locomotion develops early in life and is intrinsically linked to the behavioral ecology of the species[1,2]. Modern birds have distinct anatomical "modules" for aerial and terrestrial locomotion—wings and legs, respectively[3]—and species with greater investment in the wing module, relative to body mass, tend to have reduced investment in the leg module, and vice versa[4]. This negative relationship appears to be a performance trade-off, shaped by natural selection: longer legs increase drag in flight, and longer wings are cumbersome on land. Hyper-aerial and flightless phenotypes (e.g., Apodidae and Struthionidae, respectively) occupy the extremes of the locomotory spectrum, whereas most taxa have intermediate anatomy that may reflect an equilibrium between two selective optima[4]. Species that colonize oceanic islands with low predator density (i.e., low mortality) predictably evolve toward the hindlimb-dominated body plan, even if they never evolve to complete flightlessness[5,6]. Conversely, evolution toward the forelimb-dominated body plan is presumably caused by sources of selection (mortality) that are associated with a more volant lifestyle[7–9].

Here, we investigate the phenomenon of seasonal migration through this lens. In songbirds, migration is a complex behavioral trait, rooted in heritable genetic variation[10–14]. It is physically demanding and dangerous[8,9,15,16] and as such gives rise to new selective pressures that shape and refine morphology and physiology. Many studies have shown that long-distance migrants have longer wings, relative to body size, with higher aspect ratios and lower wing-loading than closely related short-distance migrants and sedentary species[17,18]. Instinctual behaviors are also linked to seasonal migration including migratory restlessness (*zugunruhe*) and hyperphagia, and the failure of any one of the critical components of the migratory phenotype could have fatal effects[19]. Therefore, selection-driven changes in allele frequencies may result in abrupt and/or gradual gains or losses of migratory

[1]Department of Biodiversity, Earth and Environmental Science, Drexel University, Philadelphia, PA 19103, USA. [2]Academy of Natural Sciences of Drexel University, Philadelphia, PA 19103, USA. [3]Delaware Museum of Nature & Science, Wilmington, DE 19807, USA. [4]Burke Museum of Natural History and Culture, Department of Biology, University of Washington, Seattle, WA 98105, USA. ✉email: matthewhalley@gmail.com

behavior[19–21], which could theoretically obfuscate efforts to reconstruct its evolution in a phylogenetic context[20,21]. Notwithstanding, migration-related traits have shown strong phylogenetic signal in many clades[14,18,22,23].

The genus *Catharus* (Turdidae), commonly known as nightingale-thrushes or simply thrushes, has emerged as a model system for studying the evolution of seasonal migration at multiple evolutionary scales. Despite sharing a recent common ancestor (4–6 mya), *Catharus* species exhibit an impressive array of migratory strategies[7,22,24–26]. Differing perspectives about species concepts and delimitation methods have led to conflicting taxonomies of *Catharus*, and some recent proposals have yet to be reviewed by checklist committees[27,28]. Therefore, we followed the taxonomy of the IOC World Bird List v.14.2[29] and placed contested species names in brackets. Hereafter, we use these acronyms (SED, ELM, SDM, LDM; see below) as adjectives and nouns, referring to four behavioral strategies and the species that exhibit them.

Many *Catharus* taxa are sedentary (SED) residents of montane Neotropical rainforests, like *C. maculatus*[27] and *C.* [*fuscater*] *opertaneus*[28,30]. Others, such as *C. mexicanus*, are elevational migrants (ELM) within the Neotropics[31]. At least one of these "resident" species has a mixed pattern: the northernmost populations of *C. aurantiirostris* are ELM, while the rest are apparently SED[32]. One species (*C. guttatus*), or two depending on species delimitation methods, is a short-distance migrant (SDM) within temperate North America, where it migrates latitudinally but does not cross any major (oceanic) water bodies[33–35]. Others, such as *C.* [*ustulatus*] *swainsoni*[36–38] and *C. minimus*[39,40], undertake long-distance migrations (LDM) between North and South America, with dangerous crossings of the Caribbean Sea and Gulf of México during the Atlantic hurricane season[9,16].

Even when weather conditions are ideal, an estimated 10% of *C.* [*u.*] *swainsoni* individuals perish while migrating across the Gulf of México in autumn, and the mortality rate increases to > 65% when conditions are poor[9]. In contrast, its sister group (*C.* [*u.*] *ustulatus*) takes a western (Pacific) route to Middle America, thereby avoiding the Gulf crossing[12,36]. The recent discovery that one of the LDM species (*C. fuscescens*) also practices SDM within South America, during the non-breeding season, may have implications for the origins of LDM, or it may be a derived condition[41,42]. In any case, the genetic infrastructure that supports this phenotypic diversity was presumably already present in the common ancestor of *Catharus*, because its sister group is an LDM species (*Hylocichla mustelina*) that migrates across the Gulf of México[43].

Behavioral variation of this kind makes an attractive target for phylogenetic comparative analysis, but the results of previous attempts to reconstruct the ancestral state of migration in *Catharus*[22,24–26] have been difficult to interpret. The uncertainty in the reconstructions stems from a variety of factors. First, these studies were weakened by sparse sampling of taxa and/or genetic characters. Second, the uncertain phylogenetic placement of the *C.* [*u.*] *ustulatus* + *C.* [*u.*] *swainsoni* clade, which appears to have captured the mitochondrial genome of an extinct lineage via hybridization[26,44], has led to conflicting interpretations of the evolutionary history of migration in the group. Hereafter, we refer to the hypothesis that the *C.* [*ustulatus*] clade is sister to the rest of *Catharus* as the "Delmore et al."[26] topology, although they were not the first authors to propose this arrangement[25]. Third, an unrealistically simple coding of the behavioral spectrum (migrant/resident) has failed to capture the breadth of variation in migratory strategies used by different *Catharus* taxa. For example, several taxa (e.g., *C. occidentalis*, *C. mexicanus*, *C. aurantiirostris*) were classified as "resident" (non-migratory) in previous (binary) reconstructions[22,24–26], despite evidence of ELM or even SDM in some populations[31,32,45–48].

To overcome these challenges, we generated large datasets of genomic and morphometric characters, from a nearly comprehensive taxonomic and geographic sample of *Catharus* specimens. In lieu of comparative muscle mass data from the wings and legs[4,5], which are unavailable for most taxa, we quantified the relative lengths of the forewing and tarsometatarsus, which are easily obtained from museum study skins. These variables are directly related to the inferred cause of the negative relationship between forelimb and hindlimb investment in birds (i.e., longer legs increase drag in flight; longer wings impede terrestrial movement)[4,5]. Our goals were to (1) resolve phylogenetic relationships, (2) characterize locomotory morphology as it relates to the sedentary-migratory behavioral spectrum, (3) model the evolution of migration-related morphology (i.e., the locomotory spectrum) in a phylogenetic context, and (4) reconstruct ancestral states at critical nodes of the *Catharus* phylogeny to infer evolutionary transitions in the migratory phenotype.

Results

Phylogeny and evolutionary units of analysis

We reconstructed a phylogeny with a dataset containing 156 ingroup (*Catharus*) samples and 3 outgroup (*H. mustelina*) samples (Fig. 1). The final alignment included 2,119,341 characters from 1,238 UCEs. A complete list of samples, with their associated voucher numbers and taxonomic identifications, is available in the Supplementary Material (Table S1). As explained in the Methods, we identified 25 genetically diagnosable "lineages" (i.e., monophyletic clades) that correspond unambiguously to taxonomic units with diagnosable phenotypic characters. To this, we added *C. fuscater* (sensu stricto), which has been recovered as monophyletic in previous phylogenetic analyses of mitochondrial ND2[28,49]. Thus, our comparative analysis included 26 lineages, of which 58% (15/26) were SED; 15% (4/26) were ELM; 8% (2/26) were SDM; and 19% (5/26) were LDM.

Morphological correlates of migratory behavior

We used simulation-based phylogenetic ANOVA to test whether the mean values of the wing, tail, tarsometatarsus, and "volancy" (θ = mass-equated ratio of the lengths of the wing and tarsometatarsus), obtained from adult study skins of known sex ($n = 2{,}578$), and body mass, obtained from a curated sample of publicly available records ($n = 1{,}922$), differed among migratory strategies (see Methods). Mean body mass did not differ among the strategies ($p = 0.312$), confirming its utility as a migration-independent body size proxy (Table 1). Mass-equated wing length, tarsometatarsus length, and volancy (θ), but not mass-equated tail length, were significantly different among the migratory strategies and exhibited high phylogenetic signal ($\lambda \geq 0.99$), with

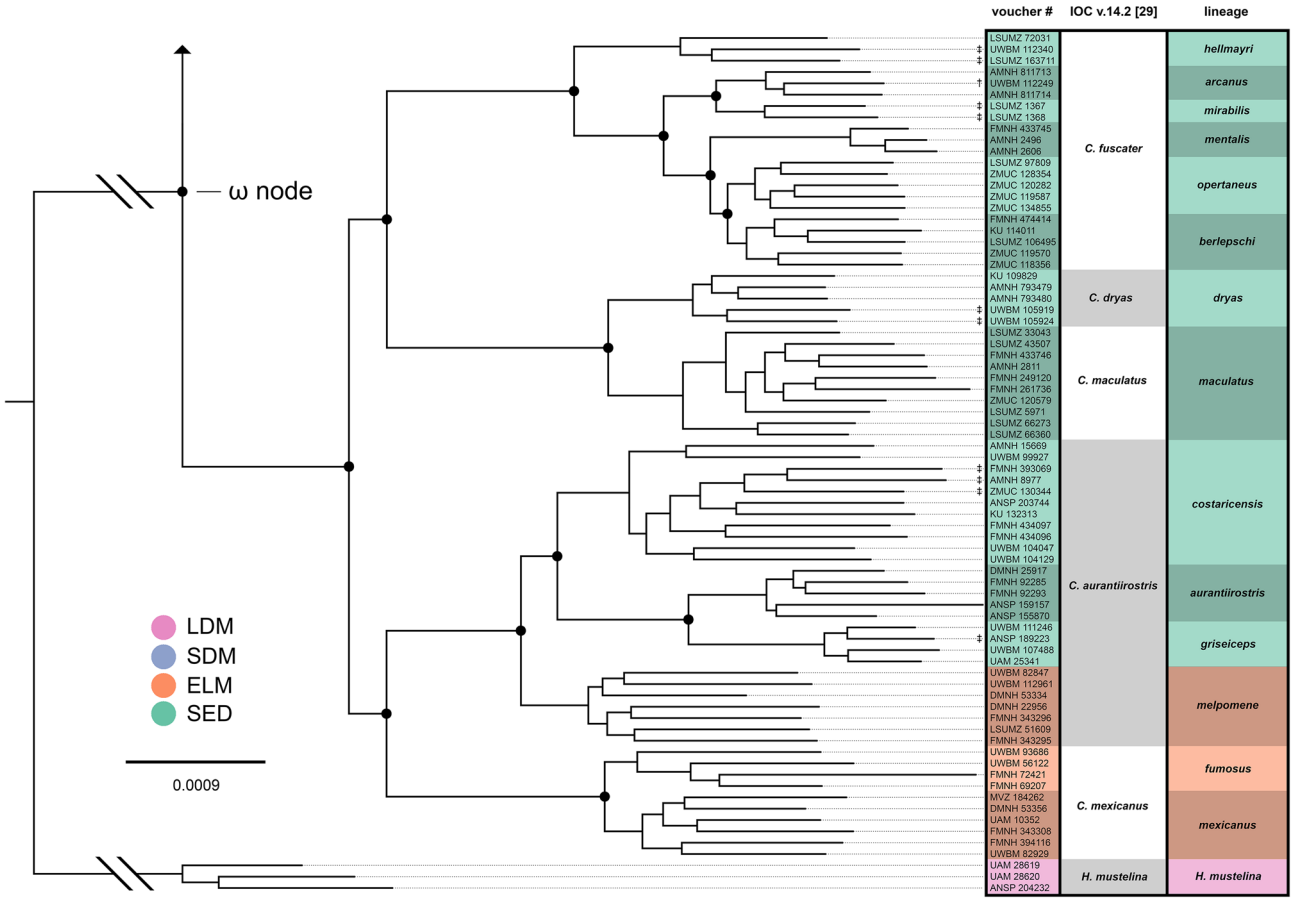

Fig. 1. Maximum likelihood (ML) phylogeny of the genus *Catharus* (Passeriformes: Turdidae) based a matrix of 1,238 UCEs assembled from 156 ingroup and 3 outgroup (*H. mustelina*) samples. Black circles denote 100% bootstrap support for nodes supporting the monophyly of lineages. The tips are denoted by (column 1) voucher number and grouped by (column 2) species limits as recognized by the IOC World Bird List v. 14.2[29] and (column 3) "lineages" recognized in this study. Colors denoting migratory strategy are standardized across figures. To the left of the voucher numbers, type specimens (i.e., supporting the lineage names) are denoted with a dagger (†) and samples collected within 50 km of a type locality ("topotypes" or nearly so) are denoted by double daggers (‡).

significant *p*-values in likelihood ratio tests (Table 1). In both sexes, the mass-equated wing and tarsometatarsus lengths had a negative relationship (Fig. 2; Linear regression, males: $p < < 0.001$, $t = -22.16$, $ß = -1.54$, df = 1,599, $R^2 = 0.24$; females: $p < < 0.001$, $t = -18.05$, $ß = -1.64$, df = 877, $R^2 = 0.27$). Mean volancy (θ) did not differ between the sexes (Fig. 3A, Mann–Whitney *U*-test, $p = 0.11$, $W = 676{,}341$) but increased progressively with migratory strategy (Fig. 3B).

Ancestral state reconstructions

We modeled the evolution of volancy (θ) by evaluating six likelihood models, separately on the UCE topology and Delmore et al.[26] topology, with two different approaches for estimating branch lengths (ND2 and EQUAL), then applied the best-fit models to reconstruct ancestral states (see Methods). The *kappa* (punctuational) model was the best fit, in the analysis that used the UCE phylogeny and ND2 branch lengths ($\kappa = 0.00$), and the *early burst* model was the best fit for the other three approaches (Table 2). In the *kappa* model, a κ-value below 1 implies that most evolutionary change is associated with cladogenesis events (at nodes), not gradual anagenesis (on branches).

Reconstructions of the common ancestor of *C.* [*guttatus*] and the LDM clade containing *C. fuscescens* (ß node, see Fig. 1) were relatively invariable, with an estimated volancy of 0.97 ± 0.01, averaged across the four approaches (reported as mean ± SD). Among the extant lineages, this estimate was closest to *C.* [*g.*] *faxoni* (SDM, $\theta_{mean} = 0.98$). The averaged upper bound (θ_{max}) of the 95% confidence interval was 1.03 ± 0.01, significantly below the means of LDM species ($\theta_{mean} = 1.06$–1.14) and *C.* [*g.*] *guttatus* (SDM, $\theta_{mean} = 1.06$). The averaged lower bound (θ_{min}) was 0.91 ± 0.01, higher than all ELM and SED lineages except *C.* [*m.*] *mexicanus* (ELM, $\theta_{mean} = 0.90$) and *C. occidentalis* (ELM, $\theta_{mean} = 0.93$). These results support an SDM or ELM ancestor at the ß node.

Reconstructions of the common ancestor of *Catharus* (ω node) were more variable and sensitive to methods. SDM was the only strategy supported by all four reconstructions. In both reconstructions with the UCE

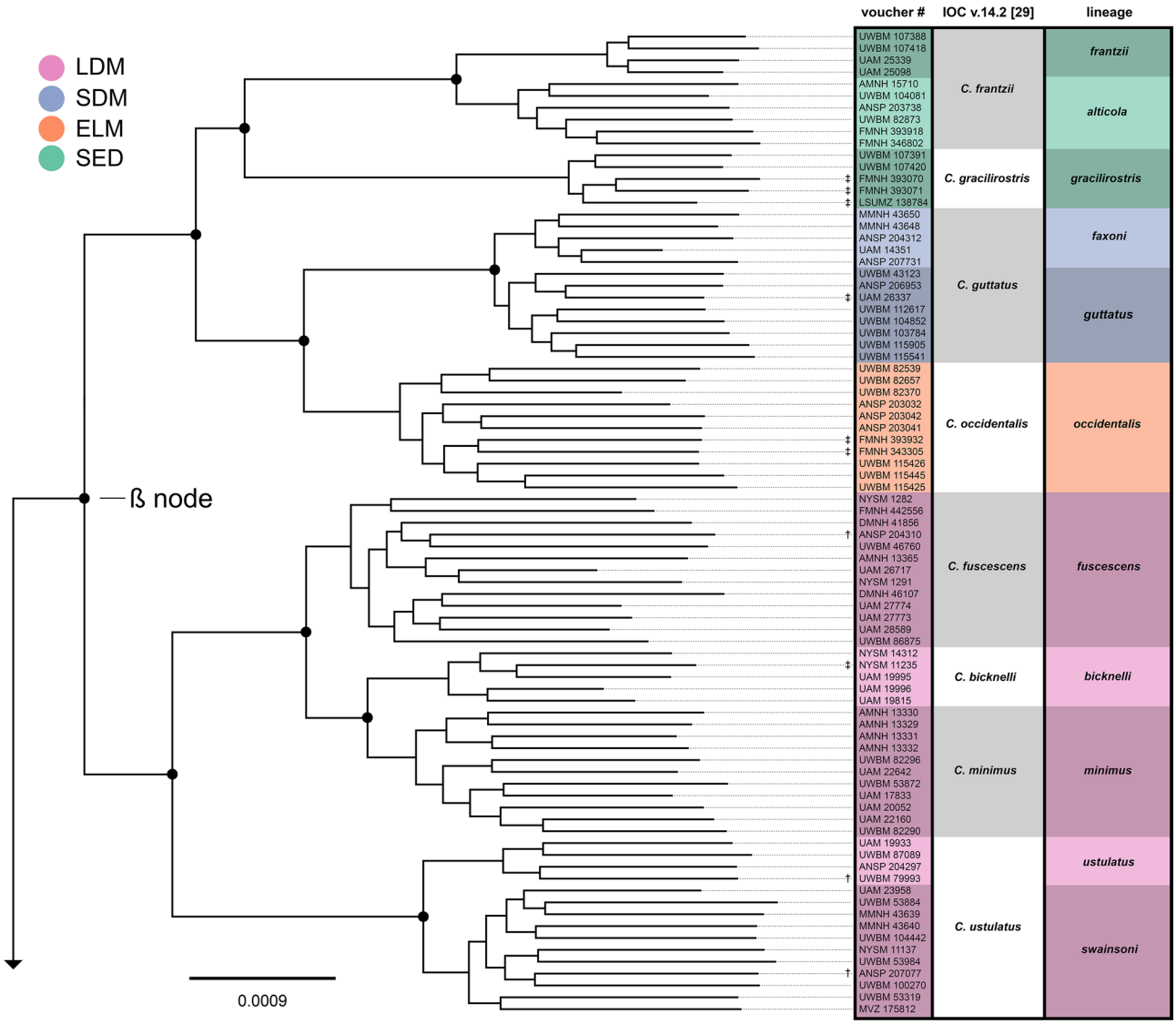

Fig. 1. (continued)

topology, the common ancestor had an estimated volancy of 0.92; the only difference was in the width of the confidence interval (ND2: 0.82–1.01; EQUAL: 0.85–0.99). Reconstructions with the UCE topology suggest that the common ancestor of *Catharus* had body proportions most similar to *C. occidentalis* (ELM, $\theta_{mean} = 0.93$), the ELM sister group of the *C.* [*guttatus*] clade. The next closest matches were *C.* [*m.*] *mexicanus* (ELM, $\theta_{mean} = 0.90$) and *C.* [*g.*] *faxoni* (SDM, $\theta_{mean} = 0.98$). The upper bound of the wider confidence interval (i.e., θ_{max} with ND2 branch lengths) was 1.01, well below the means of LDM species ($\theta_{mean} = 1.06–1.14$) and *C.* [*g.*] *guttatus* (SDM, $\theta_{mean} = 1.06$). With the UCE topology, irrespective of branch lengths, the lower bounds of the confidence intervals encompassed the values of multiple SED and ELM lineages. These results support an SDM, ELM, or SED ancestor, but not an LDM ancestor.

In reconstructions with the Delmore et al.[26] topology, where the *C.* [*u.*] *ustulatus* + *C.* [*u.*] *swainsoni* (both LDM) clade was sister to the rest of *Catharus*, the common ancestor (ω node) had an estimated volancy of 0.97, when ND2 branch lengths were used, and 1.03, when branch lengths were equal. The first estimate is most similar to *C.* [*g.*] *faxoni* (SDM, $\theta_{mean} = 0.98$). The upper bound of the confidence interval (θ_{max} averaged across the four approaches) was 1.03 (± 0.01), significantly below the means of the LDM lineages ($\theta_{mean} = 1.06–1.14$) and *C.* [*g.*] *guttatus* (SDM, $\theta_{mean} = 1.06$). The lower bound (θ_{min} averaged across the four approaches) was 0.91 ± 0.01, higher than all ELM and SED lineages except *C.* [*m.*] *mexicanus* (ELM, $\theta_{mean} = 0.90$) and *C. occidentalis* (ELM, $\theta_{mean} = 0.93$). These results support an SDM or ELM ancestor at the ω node, but not an LDM or SED ancestor.

In the final reconstruction, which used the Delmore et al.[26] topology and equal branch lengths, the common ancestor of *Catharus* had an estimated volancy of 1.03, which is higher than *C.* [*g.*] *faxoni* (SDM, $\theta_{mean} = 0.98$) but lower than any of the extant LDM lineages ($\theta_{mean} = 1.06–1.14$) and *C.* [*g.*] *guttatus* (SDM, $\theta_{mean} = 1.06$). The upper bound of the confidence interval extended to 1.10, providing weak support for an LDM ancestor, and the

Topology	Branches	Variable	λ	F	p
UCE	ND2	mass	0.90*	1.07	0.302
		WG	1.00*	23.47	**0.001**
		TR	1.00*	13.29	**0.001**
		TL	0.82*	0.24	0.827
		θ	0.99*	57.16	**0.001**
	EQUAL	mass	0.93*	1.07	0.294
		WG	1.00*	23.47	**0.001**
		TR	1.00*	13.29	**0.001**
		TL	1.00*	0.24	0.868
		θ	1.00*	57.16	**0.001**
Delmore et al.[26]	ND2	mass	0.92*	1.07	0.314
		WG	1.00*	23.47	**0.001**
		TR	1.00*	13.29	**0.001**
		TL	0.73	0.24	0.865
		θ	1.00*	57.16	**0.001**
	EQUAL	mass	0.85*	1.07	0.355
		WG	1.00*	23.47	**0.001**
		TR	1.00*	13.29	**0.001**
		TL	1.00*	0.24	0.870
		θ	1.00*	57.16	**0.001**

Table 1. Results of Phylogenetic ANOVA tests of relationships between five morphological variables (mass, WG, TR, TL, θ) and migratory strategy (independent variable with 4 classes) in the genus *Catharus* (Passeriformes: Turdidae). Four different analyses are presented for comparison, corresponding to different topologies and approaches to estimating branch lengths (see Methods). Phylogenetic signal (λ) and ANOVA test statistics (F and p-values) are provided for each variable. Asterisks (*) denote significant likelihood ratio tests ($p < 0.05$) indicating rejection of the null hypothesis of no phylogenetic signal. Bonferroni corrections were applied to all tests to control for multiple comparisons. Significant results ($p < 0.05$) are shown in boldface.

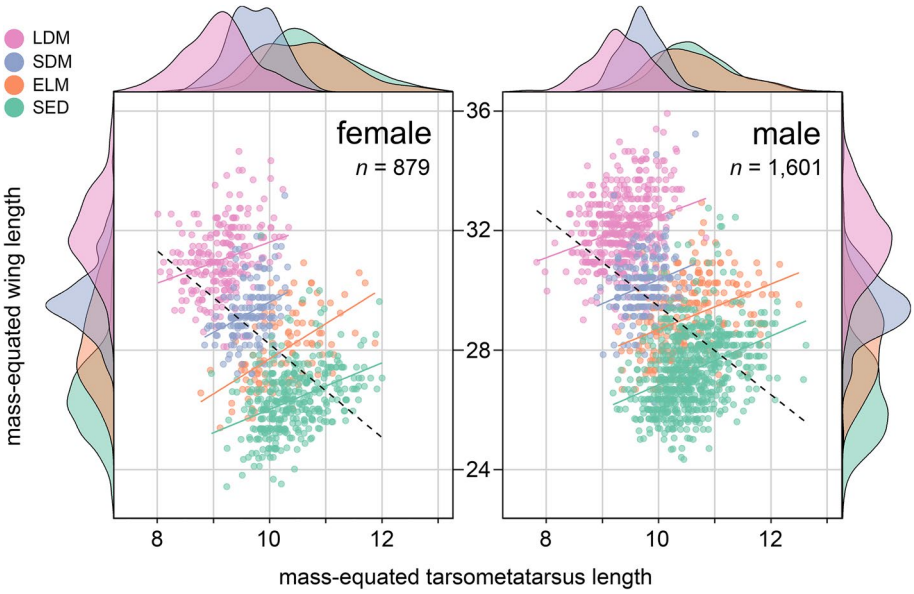

Fig. 2. Negative relationship (in both sexes) between mass-equated wing and tarsometatarsus length in the genus *Catharus* (Passeriformes: Turdidae), as measured from study skins ($n = 2{,}480$). Colors denoting migratory strategy are standardized across figures. Black dashed lines are linear regression trendlines for the female and male datasets, respectively, and colored lines are trendlines for each migratory strategy.

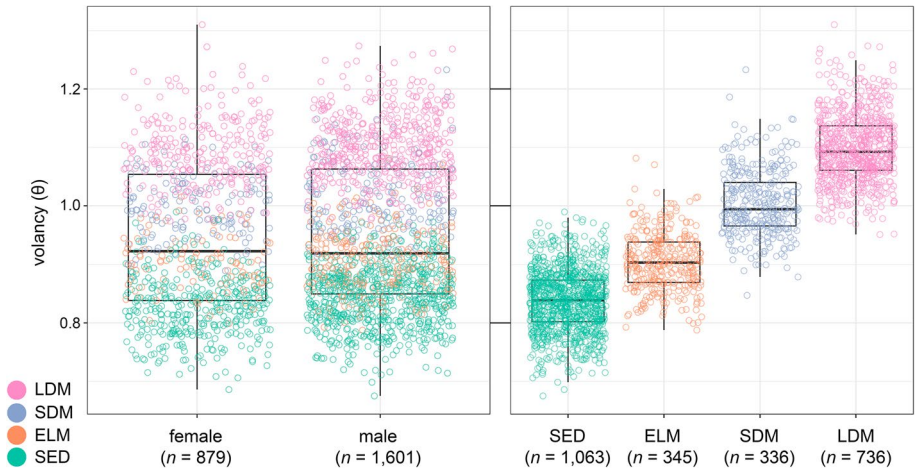

Fig. 3. Boxplots show (**A**) no relationship between sex and "volancy" (θ) in the genus *Catharus* (Passeriformes: Turdidae), based on measurements of study skins ($n = 2{,}480$); and (**B**) mean volancy increases progressively with migratory strategy (SED = sedentary; ELM = elevational; SDM = short distance; LDM = long distance). The second boxplot combines data from males and females. Colors denoting migratory strategy are standardized across figures.

Topology	Branches	Model	Node	θ_{min}	θ_{mean}	θ_{max}
UCE	ND2	kappa	ß	0.91	0.97	1.03
			ω	0.82	0.92	1.01
	EQUAL	early burst	ß	0.90	0.97	1.03
			ω	0.85	0.92	0.99
Delmore et al.[26]	ND2	early burst	ß	0.90	0.96	1.03
			ω	0.89	0.97	1.05
	EQUAL	early burst	ß	0.91	0.97	1.04
			ω	0.95	1.03	1.10

Table 2. Results of ancestral state reconstructions of "volancy" (θ) in the genus *Catharus* (Passeriformes: Turdidae), reflecting two different topologies and two approaches to estimating branch lengths. The best-fit (applied) model is shown for each reconstruction, as determined by ranking AICc scores (see Methods). The beta (ß) node represents the common ancestor of *C. guttatus* (sensu lato) and the LDM clade that contains *C. fuscescens*, *C. minimus*, and *C. bicknelli* (and *C.* [*u.*] *ustulatus* + *C.* [*u.*] *swainsoni* in the UCE topology); and the omega (ω) node represents the common ancestor of all extant *Catharus* lineages (see Fig. 1). Minimum and maximum θ-values represent the 95% confidence interval around the mean.

lower bound extended to 0.95, excluding all SED and ELM lineages ($\theta_{mean} = 0.75–0.93$). These results support an SDM or LDM ancestor at the ω node.

Discussion

By leveraging data from thousands of nuclear UCE loci, and morphometric data from thousands of museum specimens, we reconstructed a robust phylogeny of *Catharus* and confirmed that the mass-equated lengths of the forewing and tarsometatarsus, and their mass-equated ratio (volancy, θ), are statistically correlated with four behavioral strategies of increasing migratory intensity (SED > ELM > SDM > LDM). In birds, a negative relationship between forelimb and hindlimb size, as exhibited by our data, is presumably caused by performance trade-offs associated with maintaining dual (aerial and terrestrial) locomotory strategies—i.e., natural selection acting on and shaping the phenotype[4]. Our data suggest that the evolution of seasonal migration is associated with a shift toward the forelimb-dominated end of the locomotory spectrum. All four ancestral state reconstructions found support for an SDM common ancestor (ω node), while support for the other strategies (SED, ELM, LDM) was variable; and only one reconstruction found (weak) support for an LDM common ancestor [*contra* 25].

Because volancy (θ) increases progressively with migratory strategy, if directional selection (driven by non-random mortality) were to act on a SED lineage, gradually pushing it toward the forelimb-dominated end of the volancy axis, the lineage would first pass through the average ELM and SDM morphologies, before eventually arriving at the LDM morphology. If directional selection is the primary driver of volancy, as we hypothesize, this implies that species cannot rapidly "switch" between LDM and SED behavioral phenotypes (i.e., the poles

of the volancy axis), without passing through the intermediate stages [*contra* 21]. It also offers evidence that, in *Catharus* at least, SDM is an evolutionary precursor to LDM, and that the LDM clade had an SDM ancestor.

Directional selection is admittedly only one plausible explanation for the inter-lineage variation in volancy, and its correlation with migratory behavior, and we acknowledge that it may work in tandem with other macroevolutionary forces. We do not (and may never) know the role that extinction and lineage sorting played in the assembly of the extant fauna[50]. One can imagine a putative ancestral clade with a broad distribution and a range of phenotypic variation, partitioned amongst and within its populations. In such a case, the differential extinction of lineages might produce an extant fauna with a narrower and non-representative phenotypic range, relative to the ancestor, potentially misleading our reconstructions. To that point, the SDM clade (*C.* [*g.*] *guttatus* + *C.* [*g.*] *faxoni*) does have a broad geographic range and an anomalous degree of phenotypic diversity (including variation in plumage color)—"For a migratory species, the amount of geographic variation is prodigious!"[32]—although most of its geographic range is occupied solely by the trans-continental lineage *C.* [*g.*] *faxoni*, and most of the phenotypic variation is found among populations of the western lineage *C.* [*g.*] *guttatus*[32,51].

Without fossils or ancient genomic data, the scope of our evolutionary inference is obviously limited. However, our data lend credibility to a relatively novel hypothesis (with respect to *Catharus*) and warrant a discussion of its potential implications. All four ancestral reconstructions agreed that the common ancestor of the SDM and LDM clades (ß node) was most similar in volancy to *C.* [*g.*] *faxoni*. Consequently, the most parsimonious interpretation (i.e., the one requiring the smallest change in volancy) is that, since the ß node, the *C.* [*g.*] *faxoni* lineage has been in relative phenotypic stasis. We acknowledge that the characterization of an extant taxon as "ancestral" is unconventional and laden with assumptions. Notwithstanding, if our reconstructions are correct, alternative hypotheses, which fail to explain the incumbency, must nevertheless presume the existence of an extinct ancestor with a similar morphology to *C.* [*g.*] *faxoni*. The stasis hypothesis may also provide a new lens for interpreting the results of former studies. For example, if the SDM clade did not experience dramatic range contractions during the Pleistocene, like the LDM lineages[21], then the stability and breadth of its ecological niche may have buffered it against extinction, facilitating stasis.

The stasis hypothesis implies that the ecological incumbency of *C.* [*guttatus*] in North America during winter is not happenstance, but a reflection of evolutionary history—i.e., it was there first. If so, instead of multiple independent origins of migration and phenotypic convergence[24], the apparent homoplasy of the migratory phenotype (i.e., when SDM and LDM are combined as a single category) may be reflective of the occasional "budding" of daughter lineages from a long-lived stem lineage[7]. The western *C.* [*g.*] *guttatus*, which has relatively high volancy ($\theta = 1.06$) equivalent to the LDM species, may thus be viewed as the most recent daughter of the persistent SDM ancestor—a modern analog to the ancient lineage that begat the LDM clade. Similarly, *C. occidentalis* and the clade containing *C.* [*f.*] *frantzii*, *C.* [*f.*] *alticola*, and *C. gracilirostris*, would be the descendants of two additional budding events, which led to evolutionary reductions in volancy.

Finally, the stasis hypothesis has further implications for the evolution of LDM. If the ancestor of the LDM clade diverged from an ancestral SDM lineage, which persists today as *C.* [*guttatus*], then LDM may be viewed as an adaptation for winter survival in the daughter lineage, possibly driven by competitive exclusion with the parental form[52–54]. In this scenario, we hypothesize that individuals of the daughter lineage that remained in North America during winter were outcompeted by the parental SDM lineage (i.e., the ecological incumbent), but those that retreated to the south persisted and passed on the alleles that supported their migratory tendencies[7]. Because LDM across the Gulf of México and Caribbean Sea during the Atlantic hurricane season may be one of the riskiest events of the annual cycle[8,9,16,55], we must assume that the fitness cost of the alternative strategy—competing with the ecological incumbent during winter—was even greater[54]. As the non-breeding range of the LDM ancestor expanded southward, and its migrations grew progressively longer and more complex, we hypothesize that its functional morphology was gradually optimized by directional selection, driven toward the forelimb-dominated end of the volancy axis, by new sources of mortality associated with a migratory lifestyle[8,9,16].

Methods

Molecular sampling and DNA extraction

We generated DNA sequences from a taxonomically diverse collection of *Catharus* ($n = 134$) and *H. mustelina* ($n = 1$) tissues, and supplemented this dataset with sequences of *Catharus* ($n = 22$) and *H. mustelina* ($n = 2$) published by Everson et al.[43], for a total of 156 ingroup and 3 outgroup sequences (see Table S1). DNA was sourced from frozen tissues (89% of samples, 141/159) or study skin toepads (11%, 18/159). We extracted whole-genomic DNA from vouchered tissues with DNeasy tissue extraction kits following the manufacturer's protocol (Qiagen, Inc., Venlo, Netherlands). Toepad samples were collected with a sterilized scalpel and processed in a lab where no modern bird tissues have been handled. We used an extraction technique developed by Andrés M. Cuervo and colleagues[28], or a Phenol–Chloroform extraction protocol followed by bead cleanup[56]. We quantified dsDNA concentration in all extractions using a real-time qPCR fluorescent detection[57] with the Quant-iT™ PicoGreen™ dsDNA Assay Kit (Invitrogen, Eugene, OR).

UCE enrichment, sequencing and library preparation

We submitted DNA extracts to RAPiD Genomics (Gainesville, FL, USA) for library preparation and sequencing of UCEs[58]. Libraries were enriched for UCEs using either the 2.5 k tetrapod probe kit (2,386 UCEs) supplemented with approximately 100 avian exons, or the standard 5 k tetrapod probe kit (5,060 UCEs) and sequenced with either 100 (2.5 k kit) or 150 (5 k kit) base pair, paired end reads on an Illumina HiSeq 3000/4000. Mitochondrial sequence data were recovered from off target reads as a byproduct of this process[59] or with Sanger sequencing methods following Voelker et al.[25]. After sequencing, we discarded duplicate reads with the

python script fastqSplitDups.py (https://github.com/McIntyre-Lab/mcscript) and eliminated adaptors and low quality bases with trimmomatic, implemented in illumiprocessor[60–63].

We assembled the trimmed reads using ABySS 2.1.5 as implemented in PHYLUCE[59,64] following the standard UCE pipeline. PHYLUCE matched the assemblies to UCE probes and produced concatenated files for alignment. We used a series of custom scripts to create a single FASTA file containing the longest contig from each UCE (https://github.com/juliema/phylogenomics_scripts), then used this file as a new set of target sequences to readmap in aTRAM v. 2.3.0[65]. This is a pipeline that iteratively assembles reads to form contigs by first matching reads to a provided target sequence; then, for subsequent iterations, to the results from the previous iteration. We assembled contigs for each of our samples using five iterations in aTRAM v. 2.3.0 with ABySS[66]. We then selected the longest contig for each assembled UCE, grouped taxa by UCE, and aligned each UCE using MAFFT[67]. Most variation in UCEs occurs in the flanking regions rather than the central probe area, so we selected the longest contig rather than the results from the last iteration. This ensured that the maximum number of informative sites would be utilized, necessitating additional quality control steps as described below.

We verified each alignment by eye using GENEIOUS 8.0.4 (https://www.geneious.com) and performed two manual types of quality control to reduce errors caused by degraded DNA from toepad samples[68–71]. First, we removed any unalignable portions of a contig. If multiple samples had identical, but extremely divergent, sequences from other samples in the UCE probe portion of the alignment, we deleted the entire alignment from that probe. UCE probe regions from closely related samples are unlikely to exhibit large amounts of sequence variation because the probes bind to regions that are highly conserved across all tetrapods[57]. Next, we scanned (by eye) for mismatches occurring within individual toepad samples. When a column contained a base call in a toepad sample that did not occur in any other sample we re-coded the mismatches as an "N". If the base call occurred in any other sample (regardless of which sample) the base was not replaced. This final step targeted toepads because libraries prepared from toepad extracts have poorer quality reads and lower coverage than libraries prepared from frozen tissues. These extra quality control steps enabled us to reduce the "noise" caused by sequencing error and low-quality DNA in our toepad-generated sequence data, which may artificially add length and uncertainty to the inferred phylogeny. Finally, we realigned the contigs with MAFFT and trimmed the alignments with trimAL v1.2[72] to remove columns of the alignment where over half of the samples contained missing data.

Phylogenetic analysis of UCE alignment

We used Partitionfinder 2.1.1[73,74] as implemented on CIPRES[75] to select the best partitioning scheme (limited to GTR and GTR + G models) while treating each UCE as a separate partition. We selected models with the lowest second-order Akaike Information Criterion (AICc) score. Due to computational constraints we set rcluster_max to 1000 and rcluster_percent to 5.0. Because RAxML v. 8.2.12[76] as implemented on CIPRES RAxML-HPC BlackBox[75] allows only one model to be selected, we used the most commonly selected model (GTR + G) and partitioned the data in accordance with the scheme selected by Partitionfinder. We also used RAxML to perform a bootstrap analysis and allowed the program to autocomplete.

Lineage delimitation

We used "lineage" as the unit of analysis in this study, while recognizing that there is considerable disagreement about species and subspecies limits in the genus *Catharus*[27–29,32]. Following species delimitation criteria set forth in our recent revision of the *C.* [*fuscater*] complex[28], modeled after Cadena et al.[77], we identified populations as "lineages" when they were monophyletic in the UCE-derived phylogeny and had at least one diagnostic morphological or vocal character. Throughout this paper, we restrict our use of the word "lineage" to clades in our UCE phylogeny that satisfy these criteria ($n = 25$), and one polytypic species-rank clade (*C. fuscater*, sensu stricto) for which no UCE data were available[28]. All lineages recognized in this study have been previously identified as taxonomic units (Table S1) based on diagnostic characters discussed in literature[27,28,30]. Thus, our comparative analysis was based on a phylogenetic reconstruction containing 26 lineages. We used information from published literature to score each lineage with one of four migratory strategies (SED, ELM, SDM, LDM).

Branch lengths

In the comparative analysis, we used and compared two different approaches for estimating branch lengths. First, we randomly selected one sample from each of the 26 lineages and determined branch lengths via phylogenetic analysis of the mitochondrial NADH dehydrogenase subunit 2 gene (ND2). Second, because ND2 branch lengths may be unreliable in *Catharus* because of potential (ancient) gene flow among the lineages[26], we also performed separate analyses with equal branch lengths.

To determine ND2 branch lengths, we used the MUSCLE algorithm with default settings in MEGA v.11.0.13[78] to align the sequences, then imported the alignment into PAUP* 4.0a169[79] in NEXUS format. Next, we performed a heuristic search using Maximum Parsimony to produce a starting tree, followed by an automated test of 56 substitution models with Bayesian Information Criterion (BIC) to select the model with the best fit to the data. Then, we implemented the best-fit model (HKY)[80] to perform a heuristic search using Maximum Likelihood (ML) methods, while using the "constraint tree" option to restrict the output to trees that matched the topology of the UCE tree. The result was an unrooted phylogeny with 26 tips, matching the UCE topology, with branch lengths determined by ND2 distances. Then, we repeated these steps while constraining the resulting tree to the Delmore et al.[26] topology.

Morphometrics and body mass data

The lead author (MRH) used calipers and a metric ruler to record measurements from adult study skins of known sex ($n = 2{,}578$) in the collections of the American Museum of Natural History (AMNH), Academy of

Natural Sciences of Drexel University (ANSP), Carnegie Museum of Natural History (CM), Delaware Museum of Nature & Science (DMNH, formerly Delaware Museum of Natural History), Field Museum of Natural History (FMNH), Louisiana State University Museum of Natural Science (LSUMZ), Museum of Comparative Zoology, Harvard University (MCZ), and National Museum of Natural History, Smithsonian Institution (USNM). Each specimen was assigned to one of the 26 lineages based on plumage color, mandible color, and collecting locality[32].

MRH took the following three morphometric measurements, unless the body part was damaged: (1) length of the (flattened) wing, measured with a ruler (to the nearest 1 mm) from the carpal joint to the tip of the longest primary remex; (2) tarsometatarsus length, measured with calipers (to the nearest 0.01 mm) from the intertarsal joint to the distal end of the final leg scale; (3) tail length, measured with a ruler (to the nearest 1 mm) from the insertion point of the two central rectrices to the tip of the longest rectrix. All three variables were subsequently mass-equated.

To equate the variables, we downloaded *Catharus* specimen records with mass data from VertNet.org ($n = 5{,}830$) and truncated the dataset as follows. We removed mass records collected during the spring (1 April–31 May) and autumn (1 August–31 October) migratory periods, to mitigate variance caused by fluctuations in fat stores. We removed SDM and LDM females collected during the Nearctic breeding season (May–July), and ELM and SED females with at least one ovum ≥ 2 mm in diameter (based on label data), to mitigate variance caused by egg production. The truncated dataset ($n = 1{,}922$) was therefore restricted to SDM and LDM females collected during the non-breeding season (1 November–31 March), SDM and LDM males collected during the non-breeding season (1 November–31 March) and breeding season (1 June–31 July), ELM and SED females with ova ≤ 2 mm in diameter, and all ELM and SED males.

We calculated the mean body mass of each lineage and, because mass varies in proportion to the cube of the linear measurements[81], took the cube root as an index of general size. To produce our mass-equated response variables, we divided the uncorrected means of each species by the size index. Finally, for each specimen and lineage, we calculated the ratio of wing length (un-equated) to tarsometatarsus length (un-equated), then divided that value by the size index. Throughout the study, we refer to this variable as "volancy" and represent it with the Greek letter *theta* (θ).

Phylogenetic ANOVA

We used the "phylosig" function in the *phytools* package, implemented in R with RStudio[82], to estimate the phylogenetic signal (λ) of our variables[83,84] and conduct likelihood ratio tests ($\alpha = 0.05$) to determine whether the observed data were significantly different than values estimated under a null hypothesis of no phylogenetic signal. Next, we used the "phylANOVA" function to perform simulation-based phylogenetic ANOVA tests, with Bonferroni corrections for multiple comparisons, to determine whether the mean values of the response variables differed among migratory strategies.

Ancestral state reconstructions

We modeled the evolution of volancy (θ) with the "fitContinuous" function in the GEIGER library in R[85] by evaluating six likelihood models: (1) *Brownian motion*[86]; (2) *lambda*: change concentrated at the tips[84]; (3) *kappa* (punctuational): change concentrated at nodes[84]; (4) *early burst*: change concentrated at deepest nodes[85]; (5) *delta*: accelerating or decelerating[84]; and (6) *Ornstein–Uhlenbeck*: constrained random walk[87]. We used the *lambda* model to assess levels of phylogenetic signal for each variable[84], assessed model support with the second-order estimator of the Akaike information criterion (AICc), and transformed the phylogeny according to the best-fit model with functions in the GEIGER library in R[85]. Finally, we used GEIGER to reconstruct volancy values at ancestral nodes.

Data availability

All raw UCE reads generated for this project have been deposited to the NCBI SRA library (Temporary SubmissionID: SUB14752167), with a release date of "2025–10-01, or with the release of linked data, whichever is first". The morphometric data and R script are available as a supplementary file: Halley_etal_CatharusData.zip.

Received: 30 September 2024; Accepted: 9 July 2025
Published online: 17 July 2025

References

1. Darwin, C. *On the origin of species by means of natural selection, or, The preservation of favoured races in the struggle for life* (John Murray, 1859).
2. Eilam, D. Comparative morphology of locomotion in vertebrates. *J. Mot. Behav.* **27**, 100–111 (1995).
3. Gatesy, S. M. & Dial, K. P. Locomotor modules and the evolution of avian flight. *Evolution* **50**, 331–340 (1996).
4. Heers, A. M. & Dial, K. P. Wings versus legs in the avian *bauplan*: Development and evolution of alternative locomotor strategies. *Evolution* **69**, 305–320 (2015).
5. Wright, N. A., Steadman, D. W. & Witt, C. C. Predictable evolution toward flightlessness in volant island birds. *Proc. Natl. Acad. Sci.* **113**, 4765–4770 (2018).
6. Dial, K. P. & Heers, A. M. Waxing and waning of wings. *Trends Ecol. Evol.* **36**, 457–470 (2021).
7. Halley, M. R. *Integrative systematics and evolution of seasonal migration in the nightingale-thrushes (Aves: Turdidae: Catharus)* (Drexel University, 2021).
8. Sillett, T. S. & Holmes, R. T. Variation in survivorship of a migratory songbird throughout its annual cycle. *J. Anim. Ecol.* **71**, 296–308 (2002).
9. Ward, M. P. et al. Estimating apparent survival of songbirds crossing the Gulf of Mexico during autumn migration. *Proc. R. Soc. B* **285**, 20181747 (2018).
10. Berthold, P. & Pulido, F. Heritability of migratory activity in a natural bird population. *Proc. Biol. Sci.* **257**, 311–315 (1994).
11. Berthold, P. A comprehensive theory for the evolution, control and adaptability of avian migration. *Ostrich* **70**, 1–11 (1999).

12. Delmore, K. E. & Irwin, D. E. Hybrid songbirds employ intermediate routes in a migratory divide. *Ecol. Lett.* **17**, 1211–1218 (2014).
13. Justen, H. C., Easton, W. E. & Delmore, K. Mapping seasonal migration in a songbird hybrid zone—heritability, genetic correlations, and genomic patterns linked to speciation. *PNAS* **121**, e2313442121 (2024).
14. Winger, B. M., Lovette, I. J. & Winkler, D. W. Ancestry and evolution of seasonal migration in the Parulidae. *Proc. R. Soc. B* **279**, 610–618 (2012).
15. Klaassen, R. H. et al. (2013) When and where does mortality occur in migratory birds? Direct evidence from long-term satellite tracking of raptors. *J. Anim. Ecol.* **83**, 176–184 (2013).
16. Heckscher, C. M. (2018) A Nearctic-Neotropical migratory songbird's nesting phenology and clutch size are predictors of accumulated cyclone energy. *Sci. Rep.* **8**, 9899 (2018).
17. Bowlin, M. S. & Wikelski, M. Pointed wings, low wingloading and calm air reduce migratory flight costs in songbirds. *PLoS ONE* **3**, e2154 (2008).
18. Vágási, C. I. et al. Morphological adaptations to migration in birds. *Evol. Biol.* **43**, 48–59 (2016).
19. Zink, R. M. The evolution of avian migration. *Biol. J. Linn. Soc.* **104**, 237–250 (2011).
20. Helbig, A. J. Evolution of bird migration: A phylogenetic and biogeographic perspective. *Anim. Migr.* **3**, 3–20 (2003).
21. Zink, R. M. & Gardner, A. S. Glaciation as a migratory switch. *Sci. Adv.* **3**, e1603133 (2017).
22. Outlaw, D. C., Voelker, G., Mila, B. & Girman, D. J. Evolution of long-distance migration in and historical biogeography of *Catharus* thrushes: A molecular phylogenetic approach. *Auk* **120**, 299–310 (2003).
23. Gómez-Bahamón, V. et al. Speciation associated with shifts in migratory behavior in an avian radiation. *Curr. Biol.* **30**, 1312–1321 (2020).
24. Winker, K. & Pruett, C. L. Seasonal migration, speciation, and morphological convergence in the genus *Catharus* (Turdidae). *Auk* **123**, 1052–1068 (2006).
25. Voelker, G., Bowie, R. C. K. & Klicka, J. Gene trees, species trees and Earth history combine to shed light on the evolution of migration in a model avian system. *Mol. Ecol.* **22**, 3333–3344 (2013).
26. Delmore, K. E., DaCosta, J. M., & Winker, K. Thrushes in love: extensive gene flow, with differential resistance and selection, obscures and reveals the evolutionary history of a songbird clade. *Mol. Ecol.*, e17635 (2025).
27. Halley, M. R., Klicka, J., Sesink Clee, P. & Weckstein, J. D. Restoring the species status of *Catharus maculatus* (Aves: Turdidae), a secretive Andean thrush, with a critique of the yardstick approach to species delimitation. *Zootaxa* **4276**, 387–404 (2017).
28. Halley, M. R., Catanach, T. A., Klicka, J. & Weckstein, J. D. Integrative taxonomy reveals hidden diversity in the *Catharus fuscater* (Passeriformes: Turdidae) complex in Central and South America. *Zool. J. Linn. Soc.* **199**, 228–262 (2023).
29. Gill, F., Donsker, D. & Rasmussen, P. (Eds). IOC World Bird List (v14.2). https://doi.org/10.14344/IOC.ML.14.1 (2024).
30. Beltrán, W. & Kattan, G. First record of the Slaty-backed Nightingale-Thrush in the Central Andes of Colombia, with notes on its ecology and geographical variation. *Wilson Bull.* **113**, 134–139 (2001).
31. Fraser, K. C., Kyser, T. K. & Ratcliffe, L. M. Detecting altitudinal migration events in Neotropical birds using stable isotopes. *Biotropica* **40**, 269–272 (2008).
32. Phillips, A. R. *Known Birds of North and Middle America, Part 2* (Self-published, 1991).
33. Brown, D. R., Stouffer, P. C. & Strong, C. M. Movement and territoriality of wintering Hermit Thrushes in southeastern Louisiana. *Wilson Bull.* **112**, 347–353 (2000).
34. Alvarado, A. H., Fuller, T. L. & Smith, T. B. Integrative tracking methods elucidate the evolutionary dynamics of a migratory divide. *Anim. Migr.* **4**, 3456–3469 (2014).
35. Nelson, A. R. et al. Migration patterns of San Francisco Bay Area Hermit Thrushes differ across a fine spatial scale. *Anim. Migr.* **3**, 1–13 (2016).
36. Delmore, K. E., Fox, J. W. & Irwin, D. E. Dramatic intraspecific differences in migratory routes, stopover sites and wintering areas, revealed using light-level geolocators. *Proc. R. Soc. Lond. B* **279**, 4582–4589 (2012).
37. Cormier, R. L., Humple, D. L., Gardali, T. & Seavy, N. E. Light-level geolocators reveal strong migratory connectivity and within-winter movements for a coastal California Swainson's Thrush (*Catharus ustulatus*) population. *Auk* **130**, 283–290 (2013).
38. Humple, D. L. et al. Migration tracking reveals geographic variation in the vulnerability of a Nearctic-Neotropical migrant bird. *Sci. Rep.* **10**, 5483 (2020).
39. Ungvari-Martin, J., Heckscher, C. M. & Hobson, K. A. Inter-annual site fidelity and breeding origins of Gray-cheeked Thrushes in white sand forests of the Peruvian Amazon. *J. Field Ornithol.* **87**, 55–64 (2016).
40. Whitaker, D. M., Warkentin, I. G., Hobson, K. A., Thomas, P. & Boardman, R. Fall and winter movements of Newfoundland Gray-cheeked Thrushes (*Catharus minimus minimus*). *Anim. Migr.* **5**, 42–48 (2018).
41. Heckscher, C. M., Taylor, S. M., Fox, J. W. & Afanasyev, V. Veery (*Catharus fuscescens*) wintering locations, migratory Connectivity, and a revision of its winter Range using geolocator technology. *Auk* **128**, 531–542 (2011).
42. Heckscher, C. M., Halley, M. R. & Stampul, P. Intratropical migration of a Nearctic-Neotropical migratory songbird (*Catharus fuscescens*) in South America with implications for migration theory. *J. Trop. Ecol.* **31**, 285–289 (2015).
43. Stanley, C. Q. et al. Connectivity of wood thrush breeding, wintering, and migration sites based on range-wide tracking. *Conserv. Biol.* **29**, 164–174 (2014).
44. Everson, K. M. et al. Speciation, gene flow, and seasonal migration in *Catharus* thrushes (Aves: Turdidae). *Mol. Phylogenetics Evol.* **139**, 106564 (2019).
45. Collar, N. Orange-billed Nightingale-Thrush (*Catharus aurantiirostris*), version 1.0. In *Birds of the World* (eds. del Hoyo, J., Elliott, A., Sargatal, J., Christie, D. A., & de Juana, E.). Cornell Lab of Ornithology. https://doi.org/10.2173/bow.obnthr1.01 (2020).
46. Schaldach, W. J. The avifauna of Colima and adjacent Jalisco. *Mexico. Proc. West. Found. Vertebr. Zool.* **1**, 1–100 (1963).
47. Martínez-Morales, M. A. Avifauna del bosque mesófilo del noreste de Hidalgo. *México. Revista Mex. Biodivers.* **78**, 149–162 (2007).
48. Soberanes-González, C. A., Rodríguez-Flores, C. I., Arizmendi, M. d. C. & Schulenberg, T. S. Russet Nightingale-Thrush (*Catharus occidentalis*), version 1.0. In *Birds of the World* (ed. Schulenberg, T. S.). Cornell Lab of Ornithology. https://doi.org/10.2173/bow.runthr1.01 (2020).
49. Cuervo, A. M. *Evolutionary assembly of the Neotropical montane avifauna* (Louisiana State University, 2013).
50. Marshall, C. M. Five paleobiological laws needed to understand the evolution of the living biota. *Nat. Ecol. Evol.* **1**, 0165 (2017).
51. Aldrich, J. W. Population characteristics and nomenclature of the Hermit Thrush. *Proc. U.S. Nat. Mus.* **124**, 1–33 (1964).
52. Winger, B. M., Barker, F. K. & Ree, R. H. Temperate origins of long-distance seasonal migration in New World songbirds. *Proc. Natl. Acad. Sci.* **111**, 12115–12120 (2014).
53. Shaw, A. K. Drivers of animal migration and implications in changing environments. *Evol. Ecol.* **30**, 991–1007 (2016).
54. Winger, B. M., Auteri, G. G., Pegan, T. M. & Weeks, B. C. A long winter for the Red Queen: rethinking the evolution of seasonal migration. *Biol. Rev.* **94**, 737–752 (2019).
55. Lowery, G. H. Jr. Evidence of trans-Gulf migration. *Auk* **63**, 175–211 (1946).
56. Tsai, W. L. E., Schedl, M. E., Maley, J. M. & McCormack, J. E. More than skin and bones: Comparing extraction methods and alternative sources of DNA from avian museum specimens. *Mol. Ecol. Resour.* https://doi.org/10.1111/1755-0998.13077 (2019).
57. Blotta, I. et al. Quantitative assay of total dsDNA with PicoGreen reagent and real-time fluorescent detection. *Annali dell'Istituto Superiore di Sanità* **41**, 119–123 (2005).
58. Faircloth, B. C. et al. Ultraconserved elements anchor thousands of genetic markers for target enrichment spanning multiple evolutionary timescales. *Sys. Biol.* **61**, 717–726 (2012).

59. Amaral, F. S. R. et al. Ultraconserved elements sequencing as a low-cost source of complete mitochondrial genomes and microsatellite markers in non-model amniotes. *PLoS ONE* **10**, e0138446 (2015).
60. Lohse, M. et al. RobiNA: a user-friendly, integrated software solution for RNA-Seq-based transcriptomics. *Nucleic Acids Res.* **40**, W622–W627 (2012).
61. Del Fabbro, C., Scalabrin, S., Morgante, M. & Giorgi, F. M. An extensive evaluation of read trimming effects on Illumina NGS data analysis. *PLoS ONE* **8**, e85024 (2013).
62. Faircloth, B. C. illumiprocessor: a trimmomatic wrapper for parallel adapter and quality trimming. https://doi.org/10.6079/J9ILL. (2013).
63. Bolger, A. M., Lohse, M. & Usadel, B. Trimmomatic: A flexible trimmer for Illumina Sequence Data. *Bioinformatics* **30**, 2114–2120 (2014).
64. Faircloth, B. C. PHYLUCE is a software package for the analysis of conserved genomic loci. *Bioinformatics* **32**, 786–788 (2016).
65. Allen, J. M., LaFrance, R., Johnson, K. P. & Guralnick, R. P. aTRAM 2.0: An improved flexible locus assembler for NGS data. *Evol. Bioinform.* https://doi.org/10.1177/1176934318774546 (2018).
66. Jackman, S. D. et al. ABySS 2.0: Resource-efficient assembly of large genomes using a Bloom filter. *Genome Res.* **27**, 768–777 (2017).
67. Katoh, S. MAFFT multiple sequence alignment software version 7: Improvements in performance and usability. *Mol. Biol. Evol.* **30**, 772–780 (2013).
68. Axelsson, E., Willerslev, E., Gilbert, M. T. P. & Nielsen, R. The Effect of Ancient DNA Damage on Inferences of Demographic Histories. *Mol. Biol. Evol.* **25**, 2181–2187 (2008).
69. Molak, M. & Ho, S. Y. W. Evaluating the impact of post-mortem damage in ancient DNA: A theoretical approach. *J. Mol. Evol.* **73**, 244–255 (2011).
70. McCormack, J. E., Tsai, W. L. E. & Faircloth, B. C. Sequence capture of ultraconserved elements from bird museum specimens. *Mol. Ecol. Res.* **16**, 1189–2120 (2016).
71. Catanach, T. A. et al. Systematics and conservation of an endemic radiation of *Accipiter* hawks in the Caribbean islands. *Ornithology* **138**, 1–23 (2021).
72. Capella-Gutiérrez, S., Silla-Martínez, J. M. & Gabaldón, T. trimAl: A tool for automated alignment trimming in large-scale phylogenetic analyses. *Bioinformatics* **25**, 1972–1973 (2009).
73. Lanfear, R., Calcott, B., Ho, S. Y. & Guindon, S. Partitionfinder: Combined selection of partitioning schemes and substitution models for phylogenetic analyses. *Mol. Biol. Evol.* **29**, 1695–1701 (2012).
74. Lanfear, R., Frandsen, P. B., Wright, A. M., Senfeld, T. & Calcott, B. PartitionFinder 2: new methods for selecting partitioned models of evolution for molecular and morphological phylogenetic analyses. *Mol. Biol. Evol.* **34**, 772–773 (2017).
75. Miller, M. A., Pfeiffer, W. & Schwartz, T. Creating the CIPRES Science Gateway for inference of large phylogenetic trees in *Proceedings of the Gateway Computing Environments Workshop* (GCE) 1–8 (2010).
76. Stamatakis, A. RAxML version 8: A tool for phylogenetic analysis and post-analysis of large phylogenies. *Bioinformatics* **30**, 1312–1313 (2014).
77. Cadena, C. D. et al. Systematics, biogeography, and diversification of *Scytalopus* tapaculos (Rhinocryptidae), an enigmatic radiation of Neotropical montane birds. *Auk: Ornithol. Adv.* **137**, 1–30 (2020).
78. Tamura, K., Stecher, G. & Kumar, S. MEGA11: Molecular Evolutionary Genetics Analysis Version 11. *Mol. Biol. Evol.* **38**, 3022–3027 (2021).
79. Swofford, D. L. PAUP*. Phylogenetic Analysis Using Parsimony (*and Other Methods), 4.0. Sinauer Associates, (2002).
80. Hasegawa, M., Kishino, H. & Yano, T. Dating of the human-ape splitting by a molecular clock of mitochondrial DNA. *J. Mol. Evol.* **22**, 160–174 (1985).
81. Amadon, D. Bird weights as an aid in taxonomy. *Wilson Bull.* **55**, 164–177 (1943).
82. R Core Team. *R: a language and environment for statistical computing.* (R Foundation for Statistical Computing), http://www.r-project.org/index.html (accessed 14 March 2023) (2020).
83. Pagel, M. Inferring evolutionary processes from phylogenies. *Zool. Scripta* **26**, 331–348 (1997).
84. Pagel, M. Inferring the historical patterns of biological evolution. *Nature* **401**, 877–884 (1999).
85. Harmon, L. J. et al. Early bursts of body size and shape evolution are rare in comparative data. *Evolution* **64**, 2385–2396 (2010).
86. Felsenstein, J. Phylogenies and quantitative characters. *Annu. Rev. Ecol. Syst.* **19**, 445–471 (1988).
87. Butler, M. & King, A. Phylogenetic comparative analysis: A modeling approach for adaptive evolution. *Am. Nat.* **164**, 683–695 (2004).

Acknowledgements

Three anonymous reviewers provided helpful criticism of the manuscript. Early drafts were reviewed by N. H. Rice, R. M. McCourt, G. Rosenberg and J. A. Russell. Funding came from the ANSP Ornithology Department, Drexel University, the William L. McLean III Fellowship awarded to MRH, the DMNH Bird Department, and National Science Foundation (NSF) grants awarded to JDW (DEB-1855812) and TAC and JDW (DEB-2203228). Fieldwork by the lead author (MRH) was conducted under USFWS Migratory Bird Permit MB019575-1, assisted by J. Y. Sweeney and M. Gerveni. Dorothy M. Stoffa permitted MRH to collect on private property. For tissue and specimen loans, we thank S. Birks (UWBM), G. W. Shugart, D. R. Paulson (University of Puget Sound), J. Pérez-Emán (Universidad Central de Venezuela, Instituto de Zoología y Ecología Tropical and Colección Ornitolólogia Phelps), F. H. Sheldon, R. T. Brumfield, D. L. Dittmann, S. W. Cardiff, N. A. Mason, S. Pérez-Peña (LSUMZ), J. J. Kirchman (New York State Museum), R. C. K. Bowie, C. Cicero (Museum of Vertebrate Zoology, University of California Berkeley), J. Fjeldså, J. B. Kristensen (Zoological Museum, Natural History Museum of Denmark), B. D. Marks, S. J. Hackett, J. M. Bates (FMNH), M. B. Robbins (University of Kansas, Biodiversity Institute), J. L. Woods (DMNH), C. M. Heckscher (Delaware State University), J. L. Cracraft, P. R. Sweet, T. J. Trombone, B. Bird, P. Capainolo (AMNH). For collections assistance, we thank B. D. Marks, S. S. Brady, S. W. Cardiff, P. R. Sweet, B. K. Schmidt, C. M. Milensky, C. J. Dove, J. R. Saucier, N. H. Rice, J. L. Woods, and J. Trimble. For laboratory assistance, we thank J. H. Dispoto and S. Palhano. For helpful comments during our revision, we thank E. V. Griffith, J. T. Merwin, L. J. Musher, K. M. D. Kuabara, S. J. Hagler, and M. A. Pérez-Pérez. We also thank the many collectors, preparators, field assistants, and collections staff from the institutions named above and those that uploaded mass data from specimens in their care to VertNet.org.

Author contributions

The study was conceived by MRH, with guidance from JDW. Specimens were collected by all four authors. Morphometric data were collected by MRH. Genetic labwork was performed by MRH and TAC, in a space administered by JDW, or performed by JK. Bioinformatic processing was performed by TAC. Data were analyzed

by MRH and TAC. The manuscript was written by MRH, with input and edits from TAC, JK, and JDW.

Declarations

Competing interests

The authors have no competing financial and/or non-financial interests to declare in relation to this work.

Additional information

Supplementary Information The online version contains supplementary material available at https://doi.org/10.1038/s41598-025-11396-x.

Correspondence and requests for materials should be addressed to M.R.H.

Reprints and permissions information is available at www.nature.com/reprints.

Publisher's note Springer Nature remains neutral with regard to jurisdictional claims in published maps and institutional affiliations.